Jül-Conf-45 B5

I C A N S - V
MEETING OF THE INTERNATIONAL COLLABORATION ON
ADVANCED NEUTRON SOURCES
June 22-26, 1981

MODELS AND COMPUTATIONAL METHODS IN THE THEORETICAL TREATMENT OF SPALLATION NEUTRON SOURCES

T.W. Armstrong* and D. Filges

Kernforschungsanlage Jülich GmbH
Inst. f. Reaktorentwicklung
Postfach 1913
D-5170 Jülich
Federal Republic of Germany

*Consultant
P.O. Box 2807
La Jolla, California 92038, U.S.A.

Abstract:

The main aims of this review paper are: 1) to give an overview of the theoretical methods and physics models that are currently being applied in investigating various aspects of spallation neutron sources, 2) to illustrate the capabilities of present methodology with a few sample applications, and 3) to summarize some preliminary results of model validation studies that are in progress.

1. INTRODUCTION

For spallation neutron source applications, we are interested in theoretical methods that are capable of predicting a variety of different quantities related to radiation fields produced by proton beams (≈0.5 - 1 GeV) and their associated effects, both in the vicinity of the target station and from beam losses which occur in the accelerator (Table 1). It is also desirable that such calculational models be sufficiently general to allow investigations of potential applications of spallation sources for purposes in addition to providing an intense low-energy neutron source (e.g., utilization as irradiation facility for radiation effects research, high-energy nuclear physics studies, research related to transmutation and power generation, etc.) To satisfy these needs requires rather general calculational methods which can incorporate numerous physics modules for treating the various types of interaction mechanisms that take place, and which are capable of accommodating complex geometries and material configurations. This necessarily leads to large Monte Carlo computer codes, which is the type of calculational method considered in this paper.

For spallation source applications, there are basically four categories of particle interactions which must be taken into account when high-energy proton beams bombard thick targets: 1) atomic processes, 2) high-energy ($\gtrsim$15 MeV) nonelastic nuclear collisions ("spallation"), 3) pion and muon decay, and 4) the effects of low-energy ($\lesssim$15 MeV) neutron interactions. For the proton beam energy range of interest, the secondary particles produced in a single spallation collision proceed to undergo subsequent collisions, generating a multiplicity of particles inside the target material, which is illustrated schematically in Fig. 1. This process is generally referred to as a "hadronic cascade", since it is the hadrons (in this case: neutrons, protons, and charged-pions) which are effective in the "radiation transport" through the target material. The phenomenology involved has been studied previously in a number of different application areas (e.g. /1/).

Thus, we are interested in theoretical methods which can predict the details of such hadronic cascades in thick targets of various compositions and geometries. There are essentially three hadronic transport computer codes that have been written which are capable of detailed predictions: the code of Barashenkov, et al. (Dubna, USSR) /2/, the Ranft code (Karl-Marx Univ., GDR) /3/, and the HETC code /4/. In all of the current studies related to spallation neutron source facilities, HETC (or an earlier version called NMTC /5/) is the code that has been used, and it is this code which is discussed here.

Some basic features of the HETC code are summarized in Table 2. The main HETC physics models are discussed in the next section; further details can be found in /6/ and /7/.

2. MODELS AND COMPUTATIONAL METHODS

2.1 HETC Code: Physics Models

The methods used in HETC for treating atomic interactions are outlined in Table 3. These interactions are described using rather standard formulae and proceedures, and the physics uncertainties are small, so they will not be discussed in detail here.

The most difficult step in the prediction of hadronic cascades lies in determining the description (energy, angle, and multiplicity) of the secondary particles resulting from spallation collisions, and this is the source of the largest physics uncertainties in hadronic cascade predictions. In HETC, a theoretical model is used, the intranuclear-cascade-evaporation (INCE) model, in which the spallation collision is considered to proceed in two phases: 1) a "fast" phase, in which the incident particle interacts with individual nucleons inside the nucleus, producing a particle cascade inside the nucleus, and 2) a "slow" phase, in which the remaining nuclear excitation energy is distributed among all nucleons and dissipated by further

particle emission. This second phase can be described by applying a statistical evaporation model.

Intranuclear Cascade Model

The INC model, as implemented in the form of a computer code (MECC-7) by Bertini, et al. /8/ is incorporated as a subroutine in the HETC code. The major steps of the calculation are summarized in Figure 2; further details are given in /8/ and /9/.

For pion production (production threshold ~400 MeV), the Sterheimer-Lindenbaum isobar model /10/ is used, in which nucleon-nucleon or pion-nucleon collisions inside the nucleus are assumed to form an "isobar", or excited nucleon system. To determine the energy and direction of pions and nucleons emitted by the isobar, empirically determined angular distributions are specified.

The main input data required for applying the INC model are free particle-particle cross sections. Twenty-two cross sections sets, based on measured data, are input to the HETC code (Table 4). With these particle-particle cross sections and the INC model, collision products for essentially any type of target nucleus can be computed for spallation collisions which occur during the hadronic cascade. This is an important feature of the HETC calculational approach because particle-nucleus data, over the wide parameter range needed for spallation neutron source applications, is not available experimentally.

Evaporation Model

The residual mass number, charge number, and residual excitation energy after the INC are used as input for an evaporation calculation to determine further particle emission. The basic theory is that of Weisskopf /11/ as implemented by Gutherie /12/. The output of this phase of the calculation is emitted particle spectra (neutrons, protons, deuterons, tritons, ^{3}He, and alpha particles), the

type (A and Z) of residual nucleus and its recoil energy, and the final excitation energy, which is assumed to be released by γ-ray emission.

High-Energy Fission

For high energies ($\gtrsim$100 MeV) and high-mass target nuclei, there is competition between evaporation and fission at each step of the nuclear de-excitation process. For example, for collisions with uranium, fission occurs about 80% of the time at the some stage in the de-excitation chain. Statistical models can be applied to determine the parameters for the fission fragments immediately after fission, and the usual evaporation model applied to determine post-fission particle emission from each fragment (Fig. 3). Recently, several high-energy fission models have been developed for use in the HETC code /13-16/. (Calculations have recently been made at KFA to compare several of these models; this work is discussed in separate papers.)

HETC Treatment of Pion and Muon Decay

Neutral pions have a very short half-life (Table 5) and are assumed to decay at the spallation collision site where created. At the beam energies applicable for spallation neutron sources ($\lesssim$ 1 GeV), neutral pion production is small, and the decay γ-rays are normally neglected.

For charged pions "in-flight" (i.e., before coming to rest due to ionization energy losses), both decay and nuclear collisions are taken into account. Positively charged pions which come to rest are assumed to decay. Negatively charged pions which stop may be selected to decay or undergo nuclear capture, depending on the setting of an input option; the appropriate choice depends upon the density of the target material.

Pion decay in-flight is determined by defining a "macroscopic decay cross section", which is analogus to the

macroscopic cross section used for nuclear collisions (Table 5). The relative probability of decay versus collsion is then selected according to the magnitude of these two cross sections.

If the option is specified that negative charged pions become captured when stopped, the capture products are computed using the INCE model, with the initial excitation corresponding to the rest-mass energy of 140 MeV. For media containing more than one (non-hydrogen) element, the identity of the capturing nucleus is selected proportional to the electron density of the element in the mixture.

2.2 Low-Energy Neutron Transport and Analysis (10^{-5} eV-15 MeV)

The INCE model discussed above is not applicable to low-energy ($\lesssim$15 MeV) nuclear collisions. Charged particles produced $\lesssim$15 MeV in spallation collisions have short ranges and predominately come to rest before having further nuclear collisions, so usually only the low-energy neutrons produced need to be further transported. The inapplicability of the theoretical INCE model to low-energy neutron collisions is not a problem because there are large data bases of experimental nuclear cross sections available for low-energy neutrons for a wide range of target nuclei as result of extensive fission reactor and fusion research, so it is not necessary to resort to a theoretical collision model as at higher energies. Furthermore, for low-energy neutrons, there have been numerous transport computer codes developed and tested. The HETC code provides a complete descriptiion (energy, angle, and spatial distributions) of the low-energy neutrons produced in spallation collisions, which allows HETC to be coupled with any of the available low-energy transport codes.

General Requirements

A rather detailed treatment of the low-energy neutron transport is required (Table 6) since we are, in general, interested in accurate predictions of the spatial,

time, and spectral dependence. Thus, while there is some choice of low-energy transport codes which can be coupled with HETC for spallation neutron source applications, some consideration must be given to insure that the particular code and options used have the features and physics treatments for the particular results of interest.

Low-Energy Transport Codes

There are two basic types of low-energy neutron and gamma-ray transport codes that have been developed (Table 7): a) those that numerically solve the Boltzman transport equation by quadrature (discrete ordinates codes), and b) those that use stochastic methods (Monte Carlo codes). For applications where target geometries can be adequately simulated in one or two dimensions, the discrete ordinates codes usually require less computation time, especially in obtaining time-dependent results. The Monte Carlo codes are capable of simulating very complex, three dimensional target configurations. Both types of codes can be interfaced with HETC.

For the low-energy transport calculations related to the German SNQ study, the MORSE code /17/ has been used because of its general capabilities and because several useful analysis codes are available for use with MORSE. Also, MORSE is a "coupled" neutron/gamma-ray transport code-i.e., the gamma-rays created during the neutron transport from $(n,n'\gamma)$ and (n,γ) reactions are also transported, which is important for heating estimates. Other codes that have been used for spallation neutron source applications are O5R and TIMOC (at Rutherford and Appleton Laboratories for the SNS) /18,19/ and VIM (at Argonne for the IPNS).

Analysis Codes

Some features of support codes that are available for interfacing with the radiation transport codes for special analyses and results are listed in Table 8. The

SIMPEL code /20/ is a rather general analysis code that has been written at KFA to provide various results of interest from the events which occur during the HETC transport calculation.

Cross Section Codes

Cross section generation codes are used to: a) read the neutron and gamma-ray cross section data at discrete energy values from data bases and output them in a multigroup format compatible with requirements of the low-energy transport codes, and b) generate from the data bases specific "response functions" (e.g., kerma factors for obtaining energy deposition), which can then be folded with the flux spectra computed by the transport codes to obtain particular results of interest. Examples of such codes which are used at KFA are given in Table 9.

Cross Section Libraries

Evaluated cross-section data bases for neutrons and gamma-rays which are maintained at KFA and applicable to spallation neutron source applications are indicated in Table 10. For the SNQ study /21/, we have used two libraries. The EPR library has been used for energy deposition calculations since this is a coupled library and allows the heating from gamma-rays to be taken into account. However, the EPR library contains only one thermal neutron group. Therefore, for computing detailed neutron spectra from the moderators, we have used the RSYST-53 library, which has a fine group structure at low neutron energies (26 groups below 1 eV) and allows upscattering.

2.3 Summary of Calculational Proceedure

The major steps of a general calculational proceedure, using the state-of-the-art computer codes discussed above, for making theoretical estimates related to spallation neutron source applications are summarized in Fig 4, and this is the basic method that has been usd in the SNQ study /21/.

The main physics input data required are: a) particle-particle ((n,n),(n,p),(π,p),etc.) cross sections and nuclear masses for the high-energy transport, and b) low-energy (≲15 MeV) neutron and gamma-ray cross sections, which can be obtained from extensive measurements and data bases created from fission and fusion research.

Two Monte Carlo radiation transport models are used, one for the transport of high-energy (≳15 MeV) hadrons and muons and one for low-energy (≲15 MeV) neutron and gamma-ray transport. The high-energy model treats atomic interactions, particle-nucleus collisions, and particle decay. A theoretical model is used to obtain the secondary particles created in high-energy nuclear collisions, and this is the largest source of uncertainty in such predictions. While not a necessity, it is very convenient to have common geometry modules as part of both transport codes so that the same geometry and material descriptions can be used as input. For the version of the HETC code used at KFA, a "combinatorial geometry" module has been incorporated, which allows complex three dimensional target configurations to be simulated using logical commands to "combine" various simple bodies. This is the same type of geometry module contained in the standard version of the MORSE code.

The output of the transport calculations is mainly a stored data set (on disk or magnetic tape) containing a record of all "events" (nuclear collision, material boundary crossings, etc.) which occurred during each particle "history" of the Monte Carlo transport computation. Separate "analysis" codes are then used to read these data and compute various problem-dependent results of interest. While these codes are usually simple conceptually, and in a sense perform only "numerical bookkeeping" tasks, they can, in practice, be rather large and represent a substantial part of the overall programming time required.

While the method outlined in Fig. 4 is rather time consuming to carry out, both in terms of programming effort

and computer time, it has general capabilities for target and beam parameter simulation, and it can provide essentially all of the physics output quantities of interest for spallation neutron source studies.

3. EXAMPLES OF MODEL APPLICATIONS: SNQ STUDY

The calculational method described above has been applied recently as part of a German study (designated SNQ, for "Spallations Neutronen Quelle") to investigate the feasibility of spallation neutron sources for obtaining intense thermal neutron beams for solid state physics research. A report describing these calculations for the SNQ target station has recently been written /21/, and some initial results were presented previously at the ICANS-IV Meeting /22/. Here, we present only a few of these results as example applications of the models.

3.1 Target Configuration and Beam Parameters

The target configuration was simulated in the calculations as shown in Fig 5. All of the components indicated were modeled in three-dimensions, with all major material regions accounted for. The beam parameters assumed and the type of results computed are given in Table 11.

3.2 Example Results

Table 12 gives the calculated thermal flux values from the water moderator at several locations. The calculated flux value at the end of the 6 meter long beam tube has also been converted to an "equivalent isotropic flux", which is a commonly used basis for comparison in relating the neutrons measured at the end of a beam tube to the magnitude of the thermal neutron source. As indicated, the calculations predict fluxes slightly higher than the goal set for the SNQ reference design. The time -averaged thermal neutron flux in the D_2O tank (at a distance of ≈10-20 cm from the tank bottom (corresponding to the spatial maximum) is computed to be 7.0×10^{14}n cm^{-2} s^{-1} for 5mA average beam current.

While the SNQ reference design contains lead as the spallation material, a few calculations have been made for uranium also. Table 13 compares the target heating for lead and uranium for both the average energy deposition rate (i.e., time-averaged over the beam pulse structure) and the peak deposition rate (during a single pulse). For lead the average heating rate (inside the volume of the target "wheel") is about one-half of the incident beam power of 5.5 megawatts, with U-238 a factor ≈ 4 higher, and natural uranium a factor of ≈ 6 higher. The ratio of peak heating rates for uranium compared to lead are less than the ratios for the average heating rates. This is because of the different spatial distributions for the heating due to the different relative contributions of high-energy particles and low-energy neutrons.

The mass distributions for Pb and U-238 as target materials are shown in Fig. 6. These results correspond to the number of residual nuclei produced, over the total target material region, having a given mass number, and include both stable and radioactive nuclides. These results were computed using the HETC code for the high-energy spallation and fission products (incorporating the model of Atchison /13/ to obtain mass distributions of fission fragments from U-238 high-energy fissioning) and the MORSE and ORIGEN /23/ codes to obtain the mass distributions for low-energy ($\lesssim$15 MeV) fissioning. Also shown in Fig. 6 is the small amount of spallation products from the oxygen of the coolant water and the aluminum cladding contained in the target material region. The main point from Fig. 6 is that the induced radioactivity from a uraniun target is inherently larger (roughly a factor of 10) than for a lead target because of both high-energy and low-energy fissioning, and the production of particular radioactive species can be very different due to the different product mass distributions.

4. MODEL VALIDATIONS

Table 14 lists experiments that have been carried out for spallation neutron source investigations, and a brief indication of the quantities measured, target materials considered, and proton beam energies used /19,25-30/. For all of the experiments, comparisons have been made with HETC (or NMTC) code calculations; a summary of most of these comparisons is given in /21/. As part of the SNQ feasibility study, a series of experiments (Table 15) has been carried out to provide data for arriving at a reference design and to provide more extensive data for model validation. The data analyses and theoretical predictions for comparisons are not yet completed, but some preliminary comparisons have been made /21/, and a few of the results are summarized here.

Bauer, et al. /24/ have made measurements of the thermal neutrons at the end of a beam tube for 600-MeV proton bombardment using a geometry and material configuration (Table 16) which is close to the reference design model (shown previously in Fig. 5) assumed for the SNQ calculations discussed above in Section 3. For comparison with the calculations, we assume that the experiment for a 600-MeV beam energy when normalized to 10 mA beam current is approximately equivalent to the calculated beam parameters of 1100 MeV and 5 mA. (Theory and measurements show that, in this energy range, neutron production is proportional to beam energy.) A comparison of the measured and calculated thermal neutron fluxes (in terms of equivalent isotropic flux) for both H_2O and D_2O moderators is shown in Table 16. (The calculated values are the same as given previously in Table 12.) The agreement for this single comparison (within about 10%) is perhaps better than generally expected from present state-of-the-art theoretical methods. Nevertheless, this comparison provides some confidence in the calculations made for the SNQ reference design configuration model for one of the important quantities (thermal neutron output) related to assessing physics feasibility.

As part of the SNQ study, Cierjacks and co-workers of KfK have measured the neutron spectra escaping at various angles from thick, bare targets bombarded by high-energy proton beams /31/. For one case (measured spectrum at 90 degrees from a bare, cylindrical lead target 10 cm diameter and 60 cm long, 590-MeV proton beam), we have made HETC and MORSE calculations for comparison (Fig. 7). The theoretical predictions substantially underpredict the neutron spectrum at high energies (e.g., factor of about 5 at 100 MeV). (Initial comparisons with measurements of Cierjacks et al. for thin targets show a similar trend at high energies /32/) The thermal neutron fluxes in the moderators are not essentially affected by this high-energy region of the spectrum. However, high-energy neutrons are important for shielding estimates and in predicting the heating of components near the target wheel (e.g., cold-source heating). Additional calculations and comparisons are planned to try to resolve what is presently an apparently large discrepancy between theory and experiment.

Other code validation comparisons being made in the SNQ study are discussed in /21/, and a summary of the present status is given in Table 17. Also, preliminary results related to the evaluation of high-energy fission models for use in the HETC code are reported in /33/ and /34/.

5. PRESENT STATUS OF THEORETICAL MODELS FOR SPALLATION NEUTRON SOURCE APPLICATIONS

To put the present status of theoretical methods in perspective, Fig. 8 indicates the major theoretical and experimental events which have taken place. The computer codes being used today were developed some years ago, primarily for studying accelerator shielding and the shielding of manned spacecraft from cosmic radiation. However, the codes were sufficiently general to be applicable to neutron spallation source problems, and are being used for these purposes today in their original form.

Experimentally, some measurements of neutron spectra were made in the design of the WNR facility at Los Alamos, but the main experimental data for guidance in spallation source design until recently were the Cosmotron target yield data of Fraser et al. /25/, which were taken over 15 years ago. On this time scale, only rather recently have data become available from various spallation source projects to allow any extensive evaluations of the theoretical models.

To date, several theoretical/experimental comparisons have been made and definitive quantitative evaluations and weaknessess of the theory are emerging, but no modifications of the models have yet been made.

Hopefully, this research will continue to better define the theoretical uncertainties and to identify particular features of the present models which can be updated and improved. This should then allow accurate theoretical models to be applied for assessing, and optimizing, spallation neutron source performance, and to be used as reliable computational tools to aid in the engineering design and safety analyses of such facilities.

REFERENCES

1. T.W. Armstrong, "Introduction to Hadronic Cascades", Chapter 18 in Computer Techniques in Radiation Transport and Dosimetry, W.R. Nelson and T.M. Jenkins (Editors), Plenum Press, New York, (1980).

2. V.S. Barashenkov, N.M. Sobolevskii, and V.D. Toneev, "The Penetration of Beams of High-Energy Particles Through Thick Layers of Material", Atomnaya Energiya 32, 217 (1972).

3. J. Ranft, "Estimation of Radiation Problems Around High Energy Accelerators Using Calculations of the Hadronic Cascade in Matter", Particle Accelerators 3, 129 (1972).

4. T.W. Armstrong and K.C. Chandler, "HETC - A High Energy Transport Code", Nucl. Sci. and Engr. 49, 110 (1972).

5. W.A. Coleman and T.W. Armstrong, "NMTC - A Nucleon - Meson Transport Code", Nucl. Sci. and Engr. 43, 353 (1971).

6. T.W. Armstrong, "The HETC Hadronic Cascade Code", Chapter 23 in Computer Techniques in Radiation Transport and Dosimetry, W.R. Nelson and T.M. Jenkins (Editors), Plenum Press, New York, (1980).

7. T.W. Armstrong, R.G. Alsmiller, Jr., K.C. Chandler, and B.L. Bishop, "Monte Carlo Calculations of High-Energy Nucleon-Meson Cascades and Comparison with Experiment", Nucl. Sci. Engr. 49, 82 (1972).

8. H.W. Bertini, Phys. Rev. 188, 1711 (1969).

9. T.W. Armstrong, "The Intranuclear Cascade Evaporation Model", Chapter 20 in Computer Techniques in Radiation Transport and Dosimetry, W.R. Nelson and T.M. Jenkins (Editors), Plenum Press, New York, (1980).

10. R.M. Sternheimer and S.J. Lindenbaum, Phys. Rev. 123, 333 (1961).

11. V. Weisskopf, Phys. Rev. 52, 295 (1937).

12. M.P. Guthrie, "EVAP-4: Another Modification of a Code to Calculate Particle Evaporation from Excited Compound Nuclei", ORNL-TM-3119 (1970).

13. F. Atchison, "Spallation and Fission in Heavy Metal Nuclei Under Medium Energy Proton Bombardment", Proc. of Mtg. on Targets for Neutron Beam Spallation Sources (G.S. Bauer, Ed.), Jülich, W. Germany, Jül-Conf-34, (January 1980).

14. F.S. Alsmiller, et al., " Calculated Particle Production Spectra and Multiplicities from Nucleon-Fissile Element Collisions at Medium Energies", Proc. of the International Conference on Nuclear Cross Sections for Technology, Knoxville, Tennessee, (October 22-26, 1979).

15. H. Takahashi, "Fission Reaction in High-Energy Proton Cascade", Symposium on Neutron Cross-Sections from 10 to 50 MeV, Brookhaven National Laboratory, Upton, N.Y. (May 12-14,1980)

16. Y. Nakahara, "Studies of High-Energy Spallation and Fission Reactions", ICANS-IV Meeting, KEK National Laboratory for High-Energy Physics, Tsukuba, Japan (October 20-24, 1980).

17. M.B. Emmett, "The MORSE Monte Carlo Radiation Transport Code System", ORNL-4972 (1975).

18. F. Atchison, "A Theoretical Study of a Target Reflector and Moderator Assembly for SNS", Rutherford and Appleton Laboratories, RL-81-006, April 1981.

19. A.D Taylor, "Neutron Transport from Targets to Moderators", Meeting on Targets for Neutron Beam Spallation Souces (G.S. Bauer, Ed.), Julich, W. Germany, Jül-Conf-34, (January 1980).

20. SIMPEL "Analyse-Code zur Auswertung von HETC Ereignisfolgen", (KFA-Bericht in Vorbereitung).

21. T.W. Armstrong, P. Cloth, D. Filges, and R.D. Neef, "Theoretical Target Physics Studies for the SNQ Spallation Neutron Source", Jul-Spez-120, July 1981.

22. D. Filges, et al., "Theoretical Studies Related to Spallation Target Physics", Proc. of the 4th Meeting of International Collaboration on Advanced Neutron Sources (ICANS-IV), KEK National Laboratory for High Energy Physics, Tsukuba, Japan, Oct. 20-24, 1980.

23. M.J. Bell, "ORIGEN - The ORNL Isotope Generation and Depletion Code", ORNL-43628 (May 1973).

24. G.S. Bauer, "Layout of the Target Station for the German High Power Spallation Neutron Source Project", ICANS-IV Meeting, KEK National Laboratory for High Energy Physics, Tsukuba, Japan (October 20-24, 1980).

25. J.S. Fraser, et al.: "Neutron Production in Thick Targets Bombarded by High Energy Protons", Phy. in Canada 21,17 (1965).

26. G.A. Bartholomew and P.R. Tunnicliffe (Editors): "The AECL Study for an Intense Neutron-Generator (Technical Details)", Atomic Energy of Conada Limited, Chalk River, Ontario, AECL-2600, (July 1966).

27. L.R. Veeser, R.R. Fullwood, A.A. Robba, and E.R. Shunk, "Neutrons Produced by 740-MeV Protons on Uranium", Nucl. Instr. Meth. 117, 509 (1974).

28. J.M. Carpenter, et al., "Summary of Results from the ZING-P' Pulsed Neutron Source", Proc. of the 4th Meeting of International Collaboration on Advanced Neutron Sources (ICANS-IV), KEK National Laboratory for High Energy Physics, Tsukuba, Japan, Oct. 20-24, 1980.

29. G.J. Russell, et al., "Measurements of Spallation Target-Moderator Reflector Neutronics at the Weapons Neutron Research Facility", Proc. of the 4th Meeting of the International Collaboration on Advanced Neutron Sources (ICANS-IV), KEK National Laboratory for High Energy Physics, Tsukuba, Japan, Oct. 20-24, 1980.

30. P. Garvey, "Neutron Production by Spallation in Heavy Metal Targets, Experiments and Calculations", Meeting on Targets for Neutron Beam Spallation Sources (G.S. Bauer, Ed.), Jülich, W. Germany, Jül-Conf-34, (January 1980).

31. S. Cierjacks, M.T. Rainbow, M.T. Swinhoe, and L. Buth, "Messung der absoluten Ausbeuten und Spektren schneller Neutronen und sekundarer Protonen aus Spallationsreaktionen am Pb und U", Primarbericht, Kernforschungszentrum Karlsruhe (1980).

32. S. Cierjacks, et al., "High Energy Particle Spectra from Spallation Targets", ICANS-V Meeting on the International Cooperation on Advanced Neutron Sources, Jülich, W. Germany, June 22-26, 1981.

33. D. Filges et al., "High-Energy Fission Models for the HETC Code: Thick-Target Comparisons", ICANS-V Meeting on the International Cooperation on Advanced Neutron Sources, Julich, W. Germany, June 22-26, 1981.

34. T.W. Armstrong and D. Filges, "High-Energy Fission Models for the HETC Code: Thin Target Comparisons", ICANS-V Meeting on the International Cooperation on Advanced Neutron Sources, Jülich, W. Germany, June 22-26, 1981.

Table 1. Requirements of Calculational Methods

- Predictions of Interest:

  •Target Station
    neutron spectra
    heating
    activation
    shielding requirements
    material damage, etc.

  •Accelerator
    radiation fields
    component activation

  •Other
    assessments for additional potential
    applications (nuclear physics research,
    radiation effects, transmutation, etc.)

- Requires:
  general calulational methods
  (in terms output, materials, geometry,
  beam parameters)

- Which leads to:
  large Monte Carlo computer codes

Table 2. Overview of HETC Code

Name:	HETC (High-Energy Radiation Transport Code)
Particles Transported:	Neutrons (≤15 Mev), Protons, $\pi^{\pm}$, $\mu^{\pm}$
Mechanisms Included:	Ionization and Excitation Multiple Coulomb Scattering Range Straggling Pion and Muon Decay Nuclear Interactions High-Energy Fission
Calculational Method:	Monte Carlo
Nuclear Collision Model:	Intranuclear-Cascade-Evaporation
Geometry:	Three Dimensional
Materials Allowed:	Essentially Arbitrary

Table 3. Treatment of Atomic Interactions in HETC Code

- Ionization

  Bethe-Bloch Formula

- Ranges

  Numerical integration of stopping powers

- Range Straggling

  Gaussian stopping distribution

- Coulomb Scattering

  Fermi joint distribution for angular and lateral spread

  Rutherford single-scattering formula

Table 4. Cross Section Input Required for INC Model

Reactions

n-p	differential
π^+-p	absorption
π^o-p	absorption
p-p	differential
p-p	single pion production
p-p	double pion production
n-p	single pion production
n-p	double pion production
π^+-p	single pion production
π^o-p	single pion production
π^--p	single pion production
π^o-n	single pion production
π^o-p	elastic
π^o-n	elastic
π^--p	charge exchange
π^--p	elastic
p-p	elastic
n-p	elastic
π^+-p	differential
π^--p	differential
π^--p	differential charge exchange
π^o-p	differential

Energy Range

n and p reactions: 0-3500 MeV
pion reactions : 0-2500 MeV

Table 5. Pion, Muon Decay

1. Decay Properties:

particle	mean lifetime τ_0 (sec)	$c\tau_0$ (m)	decay mode
π^+	2.6×10^{-8}	7.8	$\pi^+ \rightarrow \mu^+ + \nu$
π^-	2.6×10^{-8}	7.8	$\pi^- \rightarrow \mu^- + \nu$
π^0	0.8×10^{-16}	$\sim 10^{-8}$	$\pi^0 \rightarrow \gamma + \gamma$
$\mu^\pm$	2.2×10^{-6}	~660.	$\mu^\pm \rightarrow e^\pm + \nu + \bar{\nu}$

2. HETC Treatment

	"in-flight"		"at rest"	
	collisions	decay	collisions	decay
π^+	✓	✓	–	✓
π^-	✓	✓	✓ or	✓
$\mu^\pm$	–	✓	–	✓
π^0	("immediate decay")			

3. "Decay Cross Section"

- $\tau \equiv \gamma \tau_0$, $\quad \gamma \equiv [1-(v/c)^2]^{-\frac{1}{2}}$
- $\lambda_{decay} = v\tau = v\gamma\tau_0 \equiv$ decay m.f.p

$\Longrightarrow \quad \Sigma_D(E) = 1/\lambda_{decay} \equiv$ "macroscopic decay cross section"

4. π^- Capture at Rest

- Enter INCE Routines with:
  - E_{kin} = 1 MeV
  - $E^* \approx 140$ MeV = E_0^π (π rest energy)
- Capture Nucleus:
  - $p_i \propto N_i Z_i$

Table 6. General Requirements of Low-Energy Radiation Transport Code for Spallation Neutron Sources

- Transport of neutrons and gamma-rays created in neutron collisions (coupled neutron-gamma transport)
- Anisotropic scattering
- Time dependence
- Source and eigenvalue (fission source, or combined) problems
- Solution in either the forward or adjoint mode
- Use of multigroup cross sections sets or point cross sections
- Upscattering at thermal energies
- Geometry modules same as in high energy transport and analysis (in general: three-dimensional)

Table 7. Codes Available for Low-Energy Neutron and Gamma-ray Transport

- Discrete Ordinates Codes

  (solution of Boltzmann Equation by quadrature)

  - ANISN : 1-D geomerties
  - DOT : 2-D geometries
  - TDA : time-dependent ANISN
  - TIMEX : similar to TDA

- Monte Carlo Codes

  (solution of Boltzmann Equation by stochastic methods)

  - MCNP (LASL)
  - MORSE-CG (ORNL)
  - O5R (ORNL) : earlier version of MORSE
  - TIMOC (BNL)
  - VIM (ANL)

Table 8. Support Codes for Analysis

- SIMPEL-KFA (HETC)
  - 3-D Geometry, Combinatorial
  - All particle fluxes, currents and spectra
  - Energy deposition
  - Residual nuclei distribution
  - Special options for detailed spatial analysis without new HETC runs

- MAGIC (HETC, MORSE)
  - Residual nuclei production
  - Spatial distribution of gamma sources
  - Prompt doses
  - Time-dependent gamma doses

- RECOIL (MORSE)
  - Radiation damage parameters as dpa rates and production rates (H,He)

- DOMINO (MORSE, DOT)
  - Interface between DOT-IV and MORSE for boundary source tapes

- ORIGEN (HETC, SIMPEL)
  - Depletion code for build-up and decay of HETC nuclide production rates

Table 9. Cross Section Generation Codes

- AMPX (ORNL)

  Modular system for n/γ-libraries

  from data in ENDF format

- RSYST (KFA)

  Modular system for n-libraries

  with a special 126-group thermal library

  (3.0 eV - 10^{-5} eV)

- MACK-IV (ORNL)

  Calculation of nuclear response functions

  from nuclear data in ENDF format

  (e.g., kerma factors, displacements

  (n,2n), (n,3n), (n,γ), (n,p), (n,f), etc.)

Table 10. Evaluated Cross Section Libraries

- EPR-Lib (ORNL)

  • Coupled 100-group neutron, 21-group gamma-ray cross sections (ENDF/B-IV) (14.9 MeV - 10^{-4} eV)

- THERM-126 (KFA)

  • 126-group neutron library (3.0 eV - 10^{-5} eV), with all important moderator materials

- RSYST-53 (KFA)

  • 53-group neutron library (14.9 MeV- 10^{-5} eV) with 26 neutron groups below 1 eV

- HELLO (ORNL)

  • coupled 47 neutron, 21 gamma-ray group cross section (60 MeV - 10^{-4} eV)

- VITAMIN-C (ORNL)

  • Coupled 171 neutron, 36 gamma-ray group cross sections (17.3 MeV - 10^{-4} eV)

- MACKLIB-IV (ORNL)

  • 171 neutron, 36 gamma-ray group nuclear response function library (ENDF/B-IV)

Table 11. Theoretical Predictions for SNQ Reference Design Target

- Beam Parmeters Assumed:
  - E_0 = 1100 MeV
  - $\bar{I}$ = 5 mA (3.1 x 10^{16} protons/sec)
  - $\hat{I}$ = 100 mA (6.2 x 10^{17} protons/sec)
  - Pulse Width = 0.5 milliseconds
  - Repetition Rate = 100 pulses/sec
  - Beam Profile: FWHM = 4.0 cm
- Target Model Assumed:
  - Target Composition
    - Pb : "spallation material"
    - Al : cladding
    - H_2O : coolant
  - "Hybrid" Configuration
    - D_2O: "slow" moderator
    - H_2O : "fast"moderator
  - 3-D Simulated Mockup
- Calculated Results:
  - Neutron output + γ-output
  - Heating and cooling requirements
  - Induced radioactivity
  - Radiation environments for initial estimates of:
    - Materials damage
    - Shielding

Table 12. Calculated Thermal Neutron Fluxes from Fast Moderator

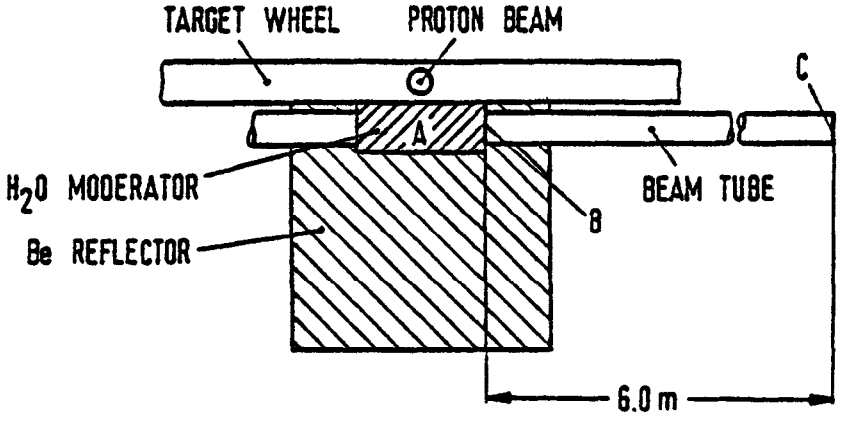

Position	Thermal Neutron Flux		
	ϕ'th (a) (n/cm^2-p)	$\bar{\phi}$th (b) (n/cm^2-s)	$\hat{\phi}$th (c) (n/cm^2-s)
A	2.0×10^{-2}	6.2×10^{14}	1.2×10^{16}
B	3.1×10^{-3}	9.7×10^{13}	1.9×10^{15}
C	2.2×10^{-7}	6.9×10^{9}	1.4×10^{11}
"EIF" (d)		7.9×10^{14}	1.6×10^{16}
"EIF" Design Goal		6.0×10^{14}	1.2×10^{16}

(a) Neutron fluence per beam proton

(b) Average neutron flux for $\bar{I}$ = 5 milliamperes

(c) Peak neutron flux for $\hat{I}$ = 100 milliamperes

(d) "EIF" = "Equivalent Isotropic Flux"

Table 13. Comparison of Heating for Lead versus Uranium as Target Material, SNQ Reference Design Geometry, 1100-MeV Protons

	Pb	U-238	Natural U
1. Total Deposition in Target (MeV)			
- HET (a)	542	945	945
- MORSE (b)	29	1140	2540
- Total	571	2085	3485
2. Total Deposition/1100 MeV	0.52	1.90	3.17
3. Total Deposition Relative to Pb	1.0	3.7	6.1
4. Peak Deposition (MeV/cm^3-proton)			
- HET (a)	1.20	2.45	2.45
- MORSE (b)	0	0.55	0.76
- Total	1.20	3.00	3.21
5. Peak Deposition (kW/cm^3), for I = 100 mA	120	300	321
6. Peak Deposition Relative to Pb	1.0	2.5	2.7

(a) From the effects of high-energy particle transport (all charged particles and neutrons > 15 MeV)

(b) From the effects of low-energy (≤15 MeV) neutron and gamma-ray transport

Table 14. Experimental/Theoretical Studies Related to Spallation Neutron Sources

1. Cosmotron Experiments (CRNL/ORNL ~1965)
   - target yields / U, Pb, Sn, Be / 540, 960, 1470 MeV

2. LASL (WNR design exp.) (Fullwood, et al., ~1971)
   - neutron spectra / bare U / 800 MeV

3. NIMROD (MUSTA experiments) (RL, late 70's)
   - neutron spectra / U + moderator + reflector /

4. Argonne (~1980)
   - neutron spectra / U + PE, H / 300, 500 MeV
   - neutron spectra / Ta, U; Pb reflector / 500 MeV
   - energy deposition / U, W / 300,500 MeV

5. FERFICON Experiments (on going)
   - target yields: U, Th, Pb, etc.
   - isotope production
     E = 480 (CRNL/TRIUMF)
     E = 800 (LASL)

6. LASL (on going)
   - E = 800 MeV
   - different neutron spectra / thin targets: U, Pb, In, Cu, Al
   - neutron spectra / moderator-reflector assemblies

7. SNQ (in progress)

Table 15. Experiments for Code Validation Related to SNQ Study

- Thin and Thick Targets
- Bare and with Moderators
- Target Materials: Mainly Pb and U
- E_0 : 600 and 1100 MeV
- Types of Measurements
  - target yields (n/p)
  - particle spectra from targets
  - neutron spatial distribution in moderators
  - time dependence of thermal flux
  - isotope production

Table 16. Theoretical / Experimental Comparisons

1. Experimental Configuration :

(Measurements of Bauer, et al. /24/)

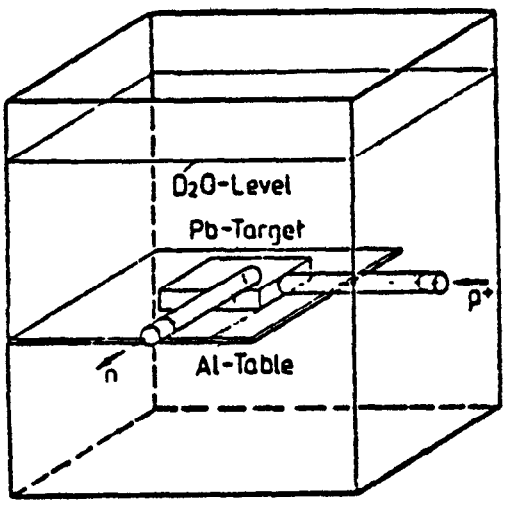

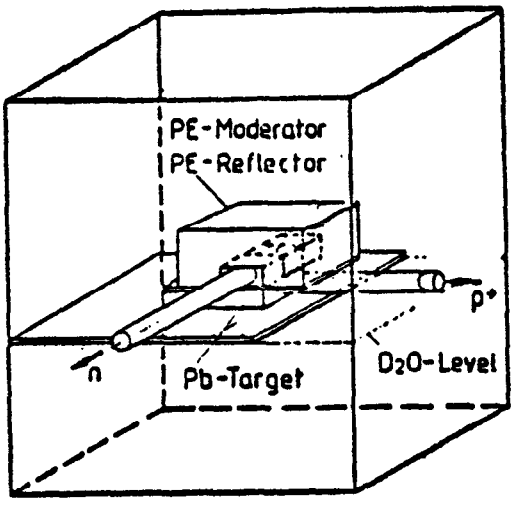

E_0 = 600 MeV

($\bar{I}$ = 10 mA)

2. Theoretical Configuration:

"Reference Design"

E_0 = 1100 MeV, $\bar{I}$ = 5 mA

3. Results

Moderator	Average Thermal Flux (n $cm^{-2}s^{-1}$)		Ratio (Theo./Exp.)
	Theory	Experiment	
D_2O	7.0×10^{14}	7.3×10^{14}	0.96
H_2O	7.9×10^{14}	7.1×10^{14}	1.11

Table 17. Experiments and Code Validations Related to SNQ Project

Case	Quantity Compared	Theoretical/Experimental Agreement
1. SNQ "Reference Design" Geometry, 600 MeV Lead Target	Thermal flux at end of beam tube	Excellent: agreement within ≈10% for both D_2O and H_2O moderators
2. "	Rh foil activation within moderators	(not yet compared)
3. SNQ "Reference Design" geometry, 600 MeV Uranium Target	Thermal flux at end of beam tube	(not yet compared)
4. "	Rh foil activation within moderators	(not yet compared)
5. Bare Pb and U, 600 and 1100 MeV	Rh foil activation	Comparisons made for 600 MeV, Pb-good agreement for relative spatial distribution (≈10-15%)
6. Pb-Bi target, H_2O moderator, 600 MeV	Spatial distribution of dysprosium reaction rate	Good agreement for relative spatial distribution (≈20%)
7. Bare Pb, 600 MeV	High-energy neutron leakage spectra, 1 MeV to 600 MeV	Poor at high energies, e.g. factor of 5 difference at 100 MeV
8. Thick Pb target 1100 MeV	Production of various isotopes of Bi, Pb, Tl and Hg	Preliminary comparisons only; Fair agreement (within factor ~2)
9. Thick U-target, 1100 MeV	Isotope production	(not yet compared)
10. Thin targets of various materials, 600 MeV	Neutron and charged particle spectra	(not yet compared)

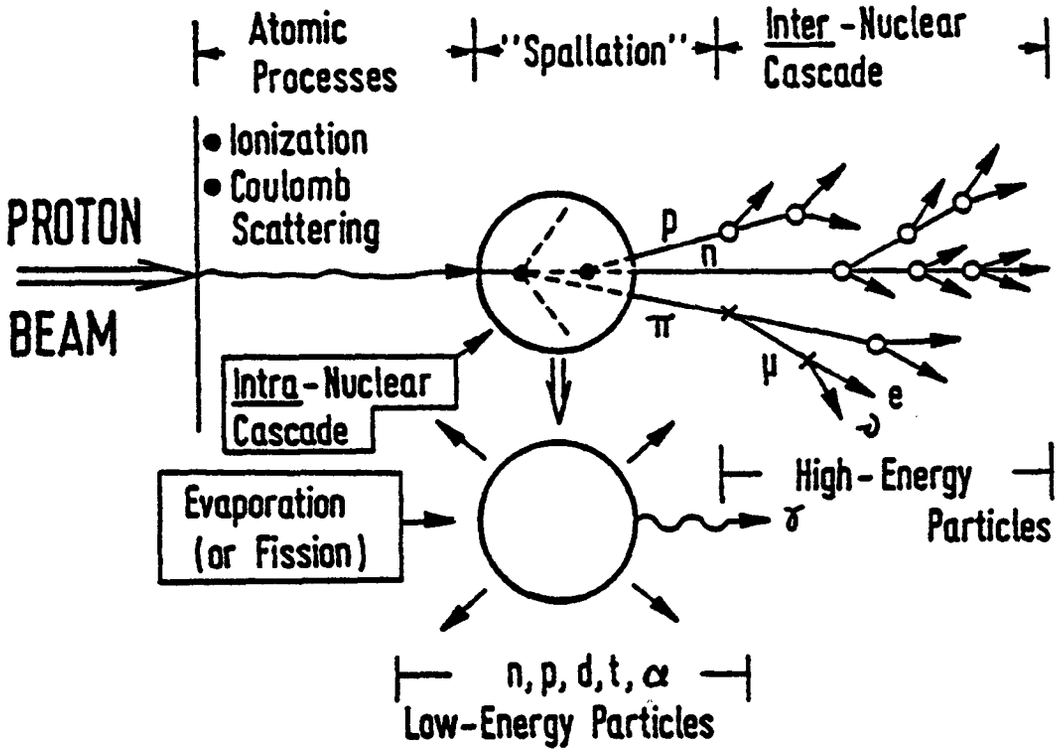

Figure 1. Interaction mechanisms produced by high-energy proton bombardment of thick targets.

Figure 2. Basic Features of Intranuclear Cascade Model Used to Treat Spallation Collisions

1. Entry into nucleus:

   -select uniformly over projected area

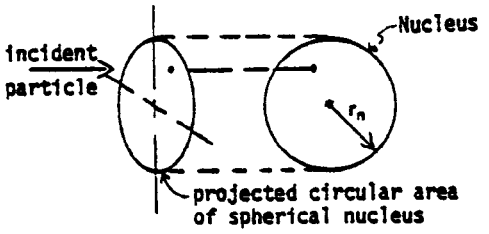

2. Nucleon Density Inside Nucleus:

   • 3-Region Approximation.

   • $[n/p]_{\text{each region}} = [(A-Z)/Z]_{\text{whole nucleus}}$

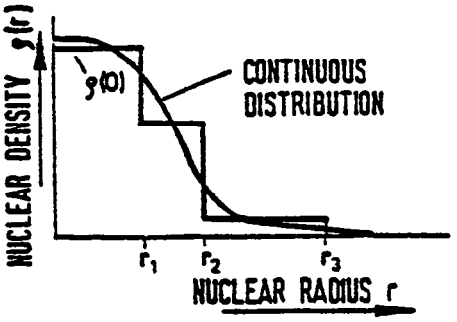

3. Nucleon Momenta:

   • Assume Fermi distribution,

   $$f(p) = cp^2$$

   • Normalization,

   $$\int_0^{p_f} f(p)\,dp = \left\{ \begin{matrix} n_i \\ p_i \end{matrix} \right\} \text{ in each region}$$

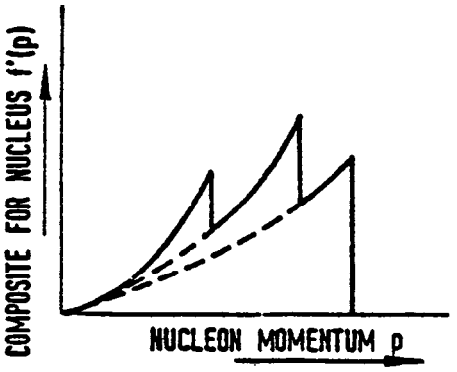

4. Nucleon Potential Energies:

   • $-V = E_f + BE$

   $BE = 7$ MeV

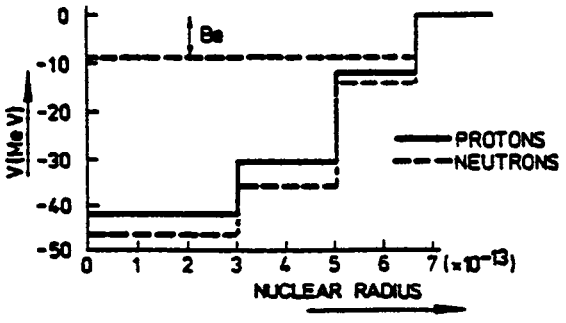

5. Cross Section Needed:

   • nucleon-nucleon
   • pion-nucleon

6. Exclusion Principle:

   -reject outcome if state filled

7. Outcome of INC:

   • $E, \overline{\Omega}$ of emitted particles: $n, p, \pi^+, \pi^\circ, \pi^-$
   • residual E^*
   • residual A, Z of nucleus

Figure 3. High-Energy Fission Model

Consider as 4-step process:

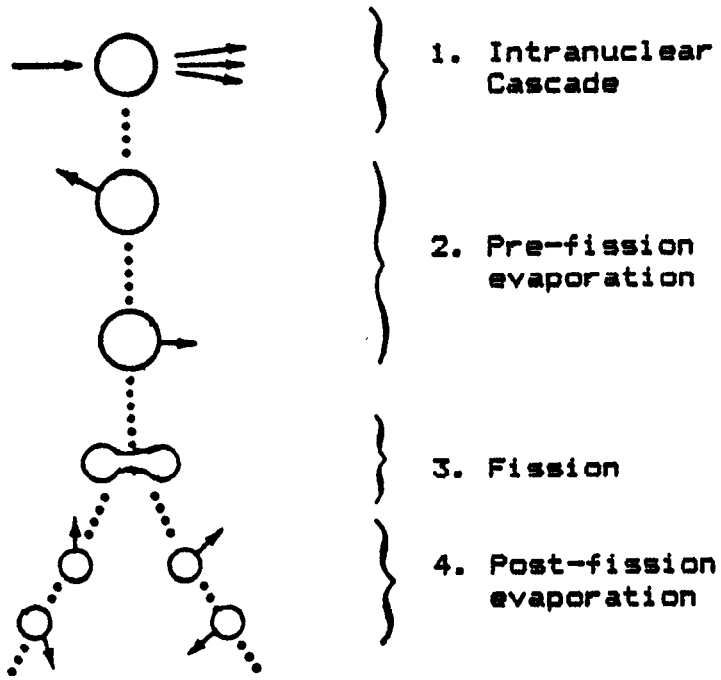

Must determine:

a. Fission probability at each step of de-excitation:

$$P_f(E^*,A,Z) \approx P_f(A,Z) \equiv (\Gamma_n/\Gamma_f + 1)^{-1}$$

b. Parameters for fission products at fission:

E_1^* , E_2^* : excitation energies

E_1 , E_2 : kinetic energies

Z_1 , Z_2 : charge numbers

A_1 , A_2 : mass numbers

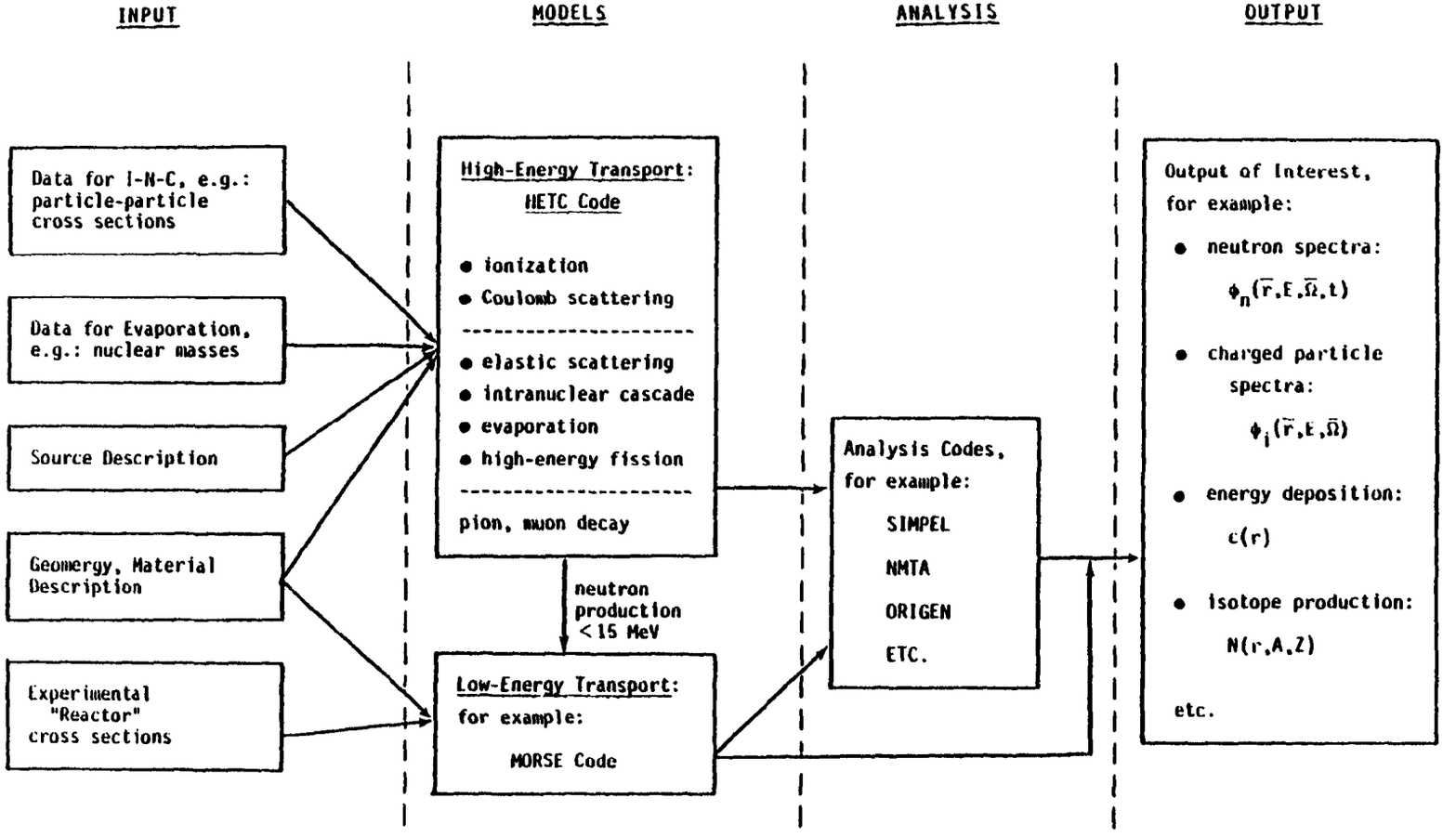

Figure 4. General Calculational Proceedure for Spallation Neutron Sources

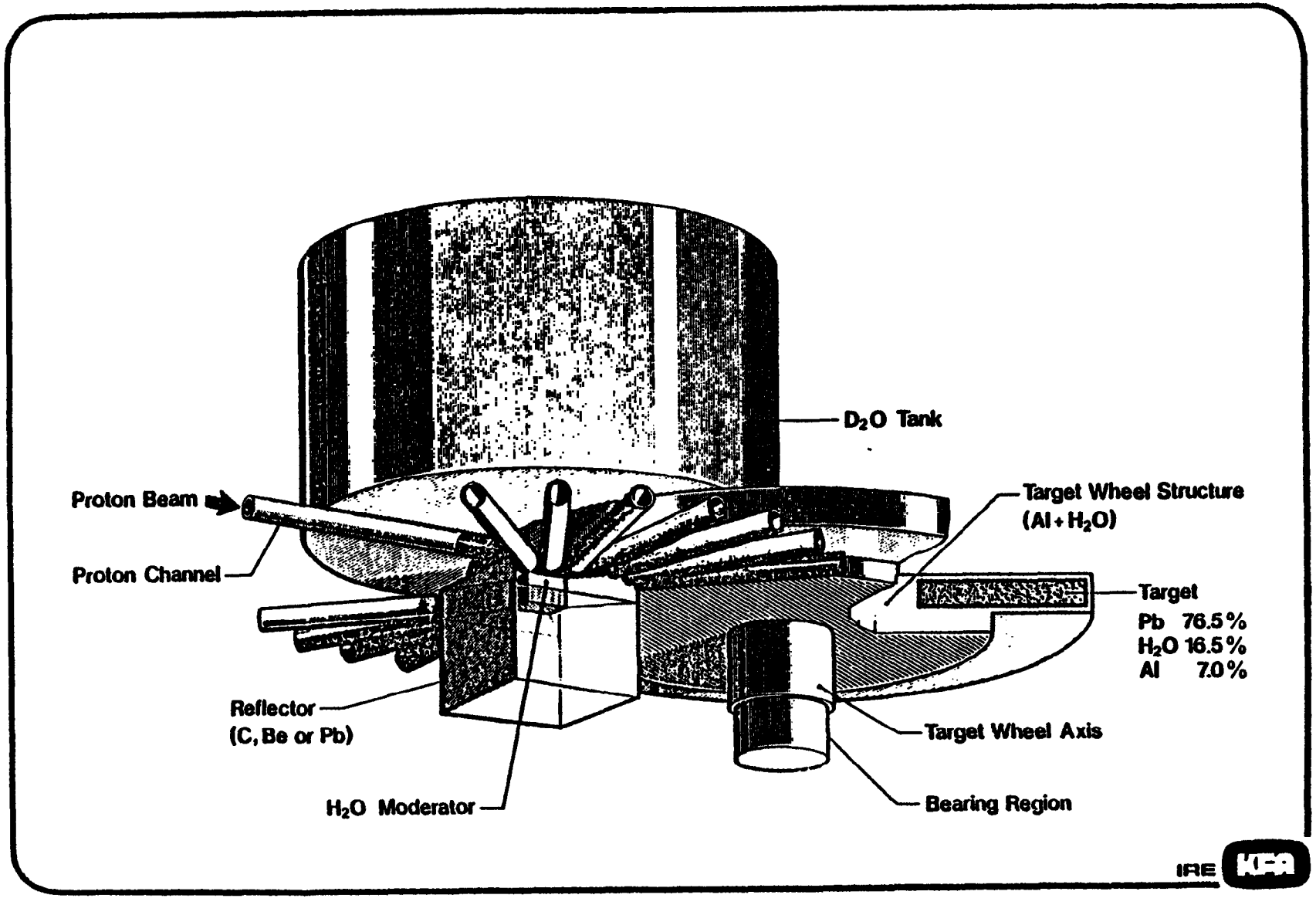

Figure 5. Three-dimensional computer model of SNQ target used for calculaions.

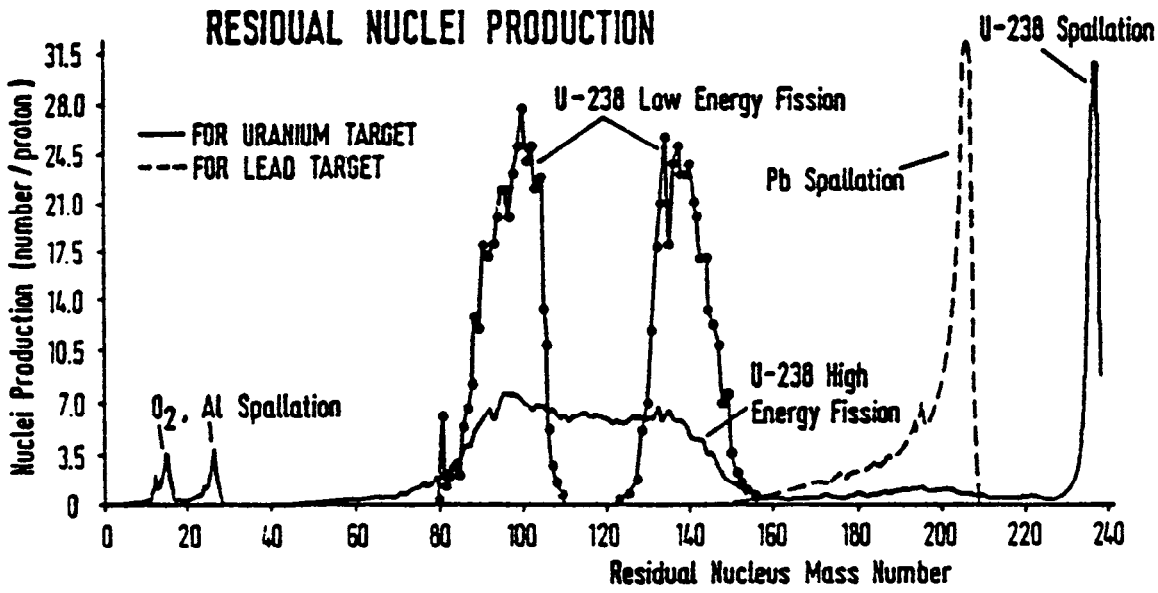

Figure 6. Mass distributions of isotopes produced for Pb and for U-238 as target materials, SNQ reference design target geometry, 1100-MeV proton beam.

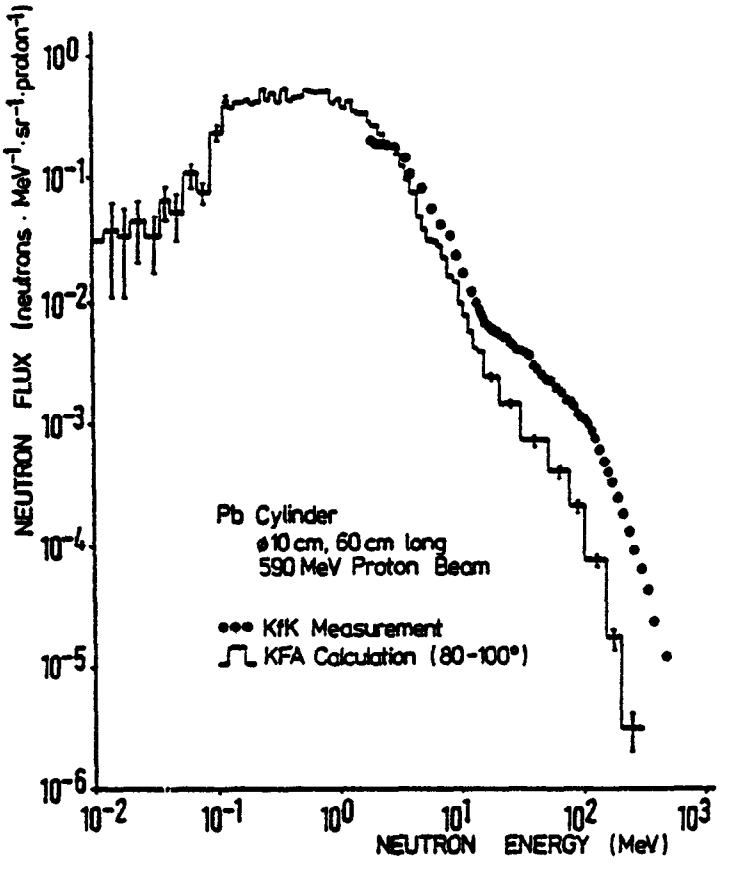

Figure 7. Comparison of calculated /21/ and measured /31/ neutron leakage spectrum at 90° (summed over 0-35 cm target length).

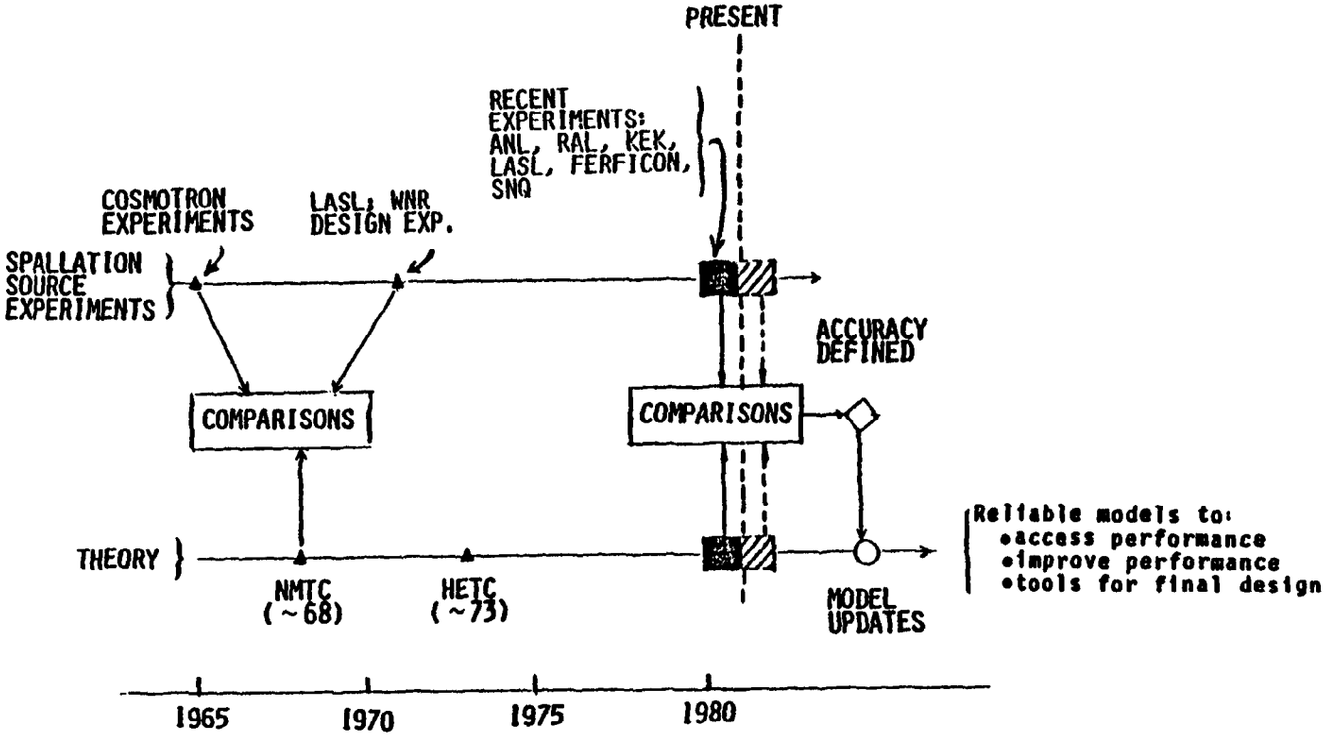

Figure 8. Present Status of Validation of Theoretical Models for Spallation Neutron Source Applications.